Journal of Information Systems Engineering and Management
2025, 10(51s)
e-ISSN: 2468-4376
https://www.jisem-journal.com/

Research Article

Metaheuristic-Based IMRT Optimization for Lung Cancer Treatment under Respiratory Motion

Keshav Kumar K.[1,3*], Dr. N.V.S.L Narasimham[2] and Dr. A. Ramakrishna Prasad[3]
[1]*Department of Humanities and Mathematics, G. Narayanamma Institute of Technology and Science (for Women), Hyderabad-500 104, Telangana State, India.*
ORCID ID: 0000-0002-9211-2960
[2]*Department of Humanities and Mathematics, G. Narayanamma Institute of Technology and Science (for Women), Hyderabad-500 104, Telangana State, India.*
ORCID ID: 0000-0002-3572-9403
[3]*Department of Mathematics, Jawaharlal Nehru Technological University, Hyderabad- 500 085, Telangana State, India.*
[*]*Corresponding Author Email: keshav.gnits@gmail.com*

ARTICLE INFO

Received: 30 Dec 2024

Revised: 15 Feb 2025

Accepted: 25 Feb 2025

ABSTRACT

Introduction: Intensity-Modulated Radiation Therapy (IMRT) is a widely adopted cancer treatment technique due to its precision in delivering radiation doses to tumors while minimizing exposure to surrounding healthy tissues. A major challenge in IMRT, however, is the movement of tumors and organs during treatment, primarily due to respiration. This motion can lead to inadequate tumor dosing or increased radiation to nearby healthy organs.

Objectives: This research aims to improve IMRT planning by incorporating motion-aware optimization techniques that account for respiratory-induced tumor and organ motion. Specifically, the study aims to identify the most effective metaheuristic optimization algorithm for enhancing IMRT performance and treatment safety.

Methods: Three metaheuristic algorithms—Genetic Bee Colony (GBC), Starling Murmuration Optimization (SMO), and Walrus Optimization Algorithm (WaOA)—were employed to optimize the IMRT objective function, which was modified to consider respiratory motion. The performance of IMRT without optimization was compared with IMRT optimized using each of these algorithms. The Dose Volume Histogram (DVH) was used as the evaluation metric to assess radiation dose distribution across the tumor and surrounding organs.

Results: Among the tested methods, the SMO-based IMRT delivered the prescribed dose of 72.7 Gy to the tumor while significantly reducing radiation exposure to critical organs such as the lung, spinal cord, and heart. Unlike unoptimized IMRT and the other two optimization techniques (GBC and WaOA), SMO demonstrated superior performance in maintaining tumor dose coverage and minimizing collateral damage.

Conclusions: The integration of the Starling Murmuration Optimization algorithm into IMRT planning offers a more effective and safer approach for treating tumors affected by respiratory motion. SMO-based IMRT enhances dose precision and reduces radiation to healthy tissues, making it a promising strategy for lung cancer therapy under motion uncertainty.

Keywords: Radiation Therapy, Optimization, Motion Uncertainty, Organ at Risk, Dose Volume Histogram

1. INTRODUCTION

Lung cancer is the leading cause of cancer-related deaths in both men and women [1]. Radiation is an important aspect of lung cancer care, as more than half of all patients receive it at some point. But the respiratory motion is a major problem in lung cancer IMRT. The movement of tumors and other organs during respiration creates significant uncertainty in target definition and therapy delivery [2]. To allow for tumor mobility, treatment margins may need to be greatly extended, increasing the risk of treatment-related damage and exposing a larger volume of normal tissue to radiation.

Conventional IMRT for lung cancer typically accounts for intrafractional tumor movement by including a margin

Journal of Information Systems Engineering and Management
2025, 10(51s)
e-ISSN: 2468-4376
https://www.jisem-journal.com/

Research Article

around the clinical target volume [3]. The term "internal target volume" (ITV) refers to the tissue inside this boundary. Due to the lack of historical data on intrafractional motion, a spatially uniform margin has generally been utilized. However, this basic definition of the ITV may be insufficient for recording tumor movements, which frequently exhibit anisotropic properties. According to studies, the extent of tumor displacement differs significantly in the superior-inferior (SI), anterior-posterior, and medial-lateral directions. For example, research [4] discovered that non-fixed tumors in the lower lobe of the lung had the highest degree of mobility, with the greatest amplitude often occurring along the SI axis.

Both patient-related variables (breathing consistency) and tumor-related factors (location and size) are likely to influence the degree of tumor motion. Clinically, it is critical to understand the correlations between the degree of tumor migration and the related ITV margin in various patient subgroups. Several studies have investigated respiration-induced tumor migration and methods for mitigating its effects, utilizing advanced technologies available at the time [5]. However, new imaging techniques have recently been developed that allow for the capture of dynamic images while breathing, thereby increasing our understanding of the kinematic and physiological characteristics of respiration. One such method, four-dimensional computed tomography (4DCT), has recently been promoted as a practical and therapeutically successful tool for measuring respiration and tumor movements.

The research focuses on optimized IMRT for lung tumors under motion uncertainty conditions, including respiration-induced motion. IMRT is optimized to improve the accuracy of dose delivery during treatment. To address the challenges posed by motion, particularly due to respiration, the objective function is designed by considering tumor motion uncertainty. The optimization techniques, such as GBC, SMO, and WaOA-based IMRT, are designed and evaluated against IMRT without optimization.

The research paper is organized as follows: Section I explains the importance of considering respiratory motion during IMRT. Section II reviews recent research works on IMRT for cancer treatment, identifies research gaps, and proposes new ideas. Section III presents the model for motion uncertainty and details the implementation of each optimization technique applied to IMRT, along with a workflow diagram. Section IV discusses the results regarding the dose delivered to both tumor and non-tumor areas. Section V concludes the research, highlighting limitations and future work.

2. OBJECTIVES

Some of the recent research work on IMRT for various tumors is analyzed and discussed in this section. The study [6] found that IMRT and Volumetric Modulated Arc Therapy (VMAT) successfully target the treatment volume for cervical cancer and deliver lower radiation doses to OARs than 3D-CRT. IMRT resulted in a far lower radiation dose than VMAT for the rectum and bladder. Both methods also significantly reduced radiation exposure to the small bowel and demonstrated superior conformance to target volumes, hence reducing harm to adjacent healthy tissues. Tumors close to vital structures are best treated with IMRT, which provides precision radiation while sparing surrounding tissue. It is preferred for high doses and sensitive organs. VMAT, on the other hand, is ideal for individuals who struggle to remain still since it simplifies planning and delivers large dosages quickly. The choice between the two is based on collaboration among the radiation oncologist, medical physicist, patient, and facility resources. A study [7] suggested using a multi-criteria optimization (MCO) technique to improve the efficiency and quality of IMRT planning for cervical cancer. Traditional IMRT planning is sometimes time-consuming due to multiple optimization steps, particularly when attempting to balance target coverage with OAR protection. The study, which included 25 patients with histologically established cervical cancer, compared traditional IMRT plans (W-IMRT) to individualized MCO-based IMRT plans (I-IMRT). The MCO technique significantly reduced radiation doses to the small bowel, bladder, rectum, and femoral heads while improving target dosage homogeneity. The findings demonstrated that MCO-based IMRT can provide more individualized therapy with superior sparing of healthy tissues, allowing for a more rapid and efficient alternative to typical individualized planning processes for cervical cancer.

This study [8] offers an interval analysis-based optimization methodology to improve the precision and resilience of IMRT, addressing the limitations of previous planning methods that rely on predetermined margins or conservative worst-case solutions. When tested on prostate cancer patients, this strategy improved tumor coverage while reducing

Journal of Information Systems Engineering and Management
2025, 10(51s)
e-ISSN: 2468-4376
https://www.jisem-journal.com/

Research Article

radiation doses to OARs, outperforming traditional Planning Target Volume and minimax techniques. The customizable parameter (θ) allows clinicians to balance robustness and conservatism based on patient needs. Despite computational challenges, increased processing power is expected to enable higher usage. The article [9] offers the Cheap-Minimax (c-minimax) model, a novel and robust optimization strategy designed for photon-based IMRT that addresses the shortcomings of traditional margin-based planning and the too conservative minimax approach. To assess its effectiveness, the c-minimax method was applied to 20 clinical cases, including 5 prostate and 15 breast malignancies. The model demonstrated superior dose sparing for OARs while maintaining or improving treatment robustness. In prostate cancer, c-minimax reduced doses to the rectum and bladder significantly when compared to minimax, whereas in breast cancer, it increased toughness while decreasing lung and heart doses. The approach also reduced high-dose exposure to surface tissues and skin, reducing potential toxicity.

The publication [10] offers a bi-level optimization strategy for IMRT for cancer treatment, with an emphasis on increasing OAR sparing while maintaining tumor coverage. The upper level of the algorithm selects beam angles that minimize radiation to healthy tissues, while the lower level optimizes radiation intensity for effective tumor treatment. The method was tested on ten head-and-neck cancer cases, using both coplanar and noncoplanar beam settings. The results showed significant improvements in treatment quality over standard seven-beam plans, with noncoplanar configurations performing best. The approach is similar to medical physicists' manual decision-making process and has the potential to improve planning. Future efforts include creating new algorithms and applying the principle to various cancer types, as well as using more advanced optimization methods such as fuzzy systems for fluence computation. The study [11] investigates the use of an Equivalent Uniform Dose (EUD)-based objective function (OF) to optimize IMRT treatment plans. EUD defines a nonuniform dose as a uniform dose with equal biological effects in both tumors and normal tissues. The study found that using EUD-based optimization for prostate and head-and-neck cancer patients resulted in similar or greater tumor coverage while conserving essential structures more effectively than normal dose-volume-based optimization. However, unless more constraints are imposed, it can result in dose inhomogeneity and hot spots in the target area. By treating the target as a virtual normal structure, dose uniformity was improved with insignificant trade-offs in OAR sparing.

From the research analysis, it is observed that IMRT not only aims to eradicate the tumor but also to minimize the radiation delivered to other organs, which is equally important. One of the major challenges in IMRT is internal organ movement due to respiration. This movement can mislead the dose distribution to the target. The research aims to design an optimized IMRT approach that accurately targets the tumor to receive the maximum dose while minimizing the dose delivered to OARs, even under respiratory motion. The research contributions are as follows:

- An objective function for IMRT in lung tumor treatment is designed by considering motion uncertainty. This helps accurately identify the target and deliver the required dosage.
- Three optimization techniques—SMO, GBC, and WaoA—are applied to IMRT to maximize the dose to the tumor and minimize the dose to OARs.
- In this research, three main organs likely to be affected during lung tumor treatment—the lung, spinal cord, and heart—are considered, and the dose delivered to these organs is analyzed.
- A comparison of the three optimization techniques with IMRT without optimization is performed to identify the most effective method for lung tumor therapy.

3. METHODS

IMRT Optimization Problem under Motion Uncertainty

The motion occurs during the IMRT, resulting in dose blurring [12]. The motion probability mass function (PMF) and static dose distribution are combined to obtain the final distribution. The dose deposition matrix can be modified before optimization (i.e., a deconvolution problem) to include motion in the planning process [13]. This guarantees that the desired distribution is achieved by convolving the static dose distribution with the motion PMF.

The designed uncertainty model uses a nominal PMF, p, with lower and upper error bars, $p + \bar{e}$ and $p - \underline{e}$, respectively. An "uncertainty region" ($U \subseteq X$) is established to specify the places where the actual PMF may differ

Journal of Information Systems Engineering and Management
2025, 10(51s)
e-ISSN: 2468-4376
https://www.jisem-journal.com/

Research Article

from the nominal one. As a result, it is assumed that the actual PMF fits the nominal PMF for the set $X\backslash U$. This paradigm enables the handling of a wide range of situations. If the breathing is exceedingly unpredictable, the nominal data are less meaningful; hence, $U = X$, and the error bars are spaced further apart. The PMF uncertainty set, P_U, is mathematically represented as shown in Equation (1):

$$P_U = \begin{Bmatrix} \tilde{p} \in \Re^{|X|} : \tilde{p}(x) \in \left[p(x) - \underline{e}(x), p(x) + \bar{e}(x)\right], \forall x \in U \\ \tilde{p}(x) \geq 0, \forall x \in X \\ \sum_{x \in X} \tilde{p}(x) = 1 \,;\, \tilde{p}(x) = p(x), \forall x \in X\backslash U \end{Bmatrix} \quad (1)$$

A formulation of the IMRT optimization problem is provided, with a solution possible for every realized $\tilde{p} \in P_U$. Next, the error bars are constructed. Let F be the PMF's family indicated by the symbols $f_0, f_1, \ldots, f_k$, with f_0 serving as the nominal PMF. Consider overlaying the upper and lower envelopes generated by each of these PMF functions on similar axes. Recall that the upper and lower error bars are represented by $p + \bar{e}$ and $p - \underline{e}$, respectively, and it is given in Equations (2 and 3). For each x, in the set X with $f_i(x) > 0$ for $i = 0, \ldots, k$, define $\bar{e}(x)$ and $\underline{e}(x)$.

$$p(x) + \bar{e}(x) = \max_{i=0,\ldots,k} f_i(x) \quad (2)$$

$$p(x) - \underline{e}(x) = \min_{i=0,\ldots,k} f_i(x) \quad (3)$$

The goal of this structure is to prevent any of the f_i from being realized during therapy and anything in between. For any $x \in X$ and $i = 0, \ldots, k$, the inequality $p(x) - \underline{e}(x) \leq f_i(x) \leq p(x) + \bar{e}(x)$ must hold. The PMF obtained from the patient will serve as the nominal PMF, and the error bars can be used in the optimization process.

The IMRT optimization challenge is defined in terms of PMF's uncertainty that describes tumor motion [14]. Consider the IMRT optimization problem as beamlet optimization without motion. Define $D_{v,b}$ as the dose received by voxel v per unit intensity of beamlet b, w_b as the beamlet's weight, and θ_v as voxel's intended or prescribed dose. Let V and B as the voxels and beamlets set are being considered, T and N be the voxels set in the tumor and non-tumor cells. The primary problem is defined as shown in Equation (4).

$$\underset{w}{minimize} \sum_{v \in V} \sum_{b \in B} D_{v,b} w_b \quad (4)$$

subject to,

$$\sum_{b \in B} D_{v,b} w_b \geq \theta_v, \quad \forall\, v \in T \quad (5)$$

$$w_b \geq 0, \forall\, b \in B \quad (6)$$

The objective is to reduce the total radiation supplied to the phantom while ensuring that all tumor voxels receive the same dose. In most circumstances, a uniform dose must be administered to the tumour; thus, $\theta_v = \theta$ for all $v \in T$.

Each voxel's nominal position is first fixed to account for motion using a PMF. Then, voxel displacement concerning this nominal reference frame is considered to create a matrix Δ, where $\Delta_{v,x,b}$ represent the dose to a voxel v by unit intensity of the beamlet b ($\Delta_{v,x,b} = D_{v,b}$ *if* $x = 0$). A PMF $p(x)$with domain X is defined, characterizing the fraction of time a voxel is displaced by x relative to its nominal position, to compute the motion-averaged dosage to a voxel v from beamlet b.

$$\sum_{x \in X} \Delta_{v,x,b}\, p\,(x) \quad (7)$$

The problem can be rephrased to include motion as given in Equations (8,9,10):

$$minimize_w \sum_{v \in V} \sum_{b \in B} \sum_{x \in X} \Delta_{v,x,b}\, p(x) w_b \quad (8)$$

subject to

$$\sum_{b \in B} \sum_{x \in X} \Delta_{v,x,b}\, p(x) w_b \geq \theta_v \quad \forall v \in T \quad (9)$$

$$w_b \geq 0 \quad \forall\, b \in B \quad (10)$$

Journal of Information Systems Engineering and Management
2025, 10(51s)
e-ISSN: 2468-4376
https://www.jisem-journal.com/

Research Article

The preceding approach considers rigid-body motion; therefore, the problem can be extended to non-rigid motion by assigning a potentially unique PMF, $p_v(x)$, to each voxel v. The model of uncertainty is now provided, leading to the following significant concern as given in Equations (11,12,13).

$$minimize_w \sum_{v\in V} \sum_{b\in B} \sum_{x\in X} \Delta_{v,x,b}\, p(x) w_b \qquad (11)$$

subject to

$$\sum_{b\in B} \sum_{x\in X} \Delta_{v,x,b}\, \tilde{p}(x) w_b \geq \theta_v \; \forall v \in T \qquad (12)$$

$$w_b \geq 0 \qquad \forall\, b \in B \qquad (13)$$

According to the OF, if the patient breathes by p, the integral dosage to the phantom is minimized. The ambiguity in the restrictions is the main focus here. In other words, resilience is necessary against any uncertainty that may prevent the tumor's voxels from receiving at least the recommended dosage. Equation (14) can be stated equivalently; however, it contains an unbounded number of restrictions because the set P_U includes an unbounded number of entries.

$$minimize_w \sum_{v\in V} \sum_{b\in B} \sum_{x\in X} \Delta_{v,x,b}\, p(x) w_b \qquad (14)$$

subject to

$$\sum_{b\in B} \sum_{x\in X} \Delta_{v,x,b}\, p(x) w_b + \beta_v(w) \geq \theta_v \quad \forall v \in T \; (15)$$

$$w_b \geq 0 \quad \forall\, b \in B \qquad (16)$$

where,

$$\beta_v(w) = min_{\hat{p}} \sum_{b\in B} \sum_{x\in U} \Delta_{v,x,b} \hat{p}(x)\, w_b \qquad (17)$$

subject to

$$\sum_{x\in U} \hat{p}(x) = 0 \qquad (18)$$

$$-\underline{e}(x) \leq \hat{p}(x) \leq \bar{e}(x) \qquad \forall\, x \in U \qquad (19)$$

Metaheuristic Algorithm for Optimization

The three optimization techniques inspired by biological processes are applied to optimize IMRT. The optimization techniques used in this research are SMO, GBC, and WaoA. The working principles of these three algorithms are discussed in this section.

A. Starling Murmuration

Starling murmuration is an impressive display of group behavior, where large flocks of starlings fly together in smooth, coordinated patterns, creating shifting shapes in the sky that look like moving clouds [15]. The reasoning behind adopting this behavior in optimization is that none of the several birds flying in tandem ever collide with one another. It is no surprise that one of the earliest real-world uses of the SMO algorithm was to manage the coordinated flight of large groups of drones. The SMO introduces three novel search techniques: separating, diving, and whirling [16]. The working of SMO is shown in Figure 1.

Journal of Information Systems Engineering and Management
2025, 10(51s)
e-ISSN: 2468-4376
https://www.jisem-journal.com/

Research Article

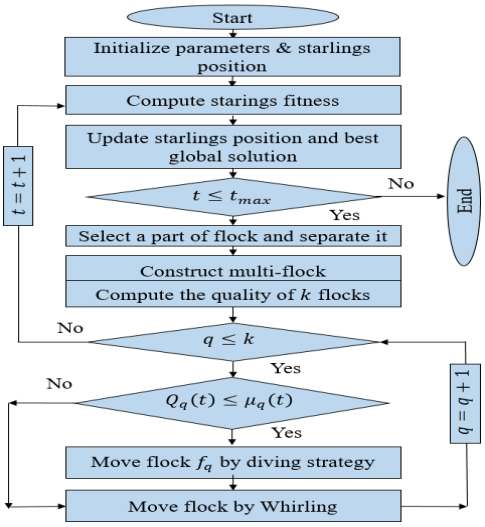

Fig. 1. *Workflow of Starling Murmuration*

Individual starlings are distributed randomly in the method's initial stages. The earlier position of the i-th starling in the group is given as in Equation (20):

$$x_{id} = x_d^L + rand(0,1)(x_d^U - x_d^L) \qquad (20)$$

where, N represents the total starlings, D represents the total dimensions in the search area, and x_{id} represents the d-th dimension of the starling. x_d^U and x_d^L represents the search area's upper and lower bounds. $rand(0,1)$ represents the random function.

Following initialization, some of the starlings depart the flock to establish a new flock, P_{sep}, which will investigate the search area as shown in Equation (21):

$$P_{sep} = \frac{log(t+D)}{2\log(t_{max})} \qquad (21)$$

Where, t represents the current iteration number and t_{max} represents the maximum iterations. The searching is given in Equation (22):

$$X_i(t+1) = X_G(t) + [\asymp]_1(y)[X_{r'}(u) - X_r(t)] \quad (22)$$

where $X_G(t)$ denotes the global location acquired during the iterative step t, and $X_{r'}(t)$ denotes the position obtained from a portion of the split flock and the fittest starlings. A new operator based on the classical quantum harmonic oscillator is the separation operator $[\asymp]_1(y)$, where y represents the random number.

The multi-flock, which consists of members $f_1, f_2, \ldots, f_k$, is dynamically formed by the starlings that survived after the split. To decide whether to employ the exploration (diving) or exploitation (whirling) search methods, the quality $Q_q(t)$ of the q-th flock is calculated using Equation (23):

$$Q_q(t) = \frac{\sum_{i=1}^{k}\sum_{j=1}^{n} sf_{i,j}(t)}{\frac{1}{n}\sum_{i=1}^{n} sf_{qi}(t)} \qquad (23)$$

While the whirling technique utilizes a new force operator to exploit the proximity of favorable areas, the diving approach uses a novel quantum random dive operator to search the search area. $sf_{ij}(t)$ represents the fitness value of the i-th starling from the j-th flock f_j, and k represents the total flocks in a murmuration M. μ_q represents the measure of the average flock's quality [17].

Journal of Information Systems Engineering and Management
2025, 10(51s)
e-ISSN: 2468-4376
https://www.jisem-journal.com/

Research Article

B. Genetic bee colony (GBC) algorithm

The intelligent swarm method for food detection and collection in genetic bee colonies [18]. Communication links, mating, task allocation, dance, reproduction, and mobility are employed to identify the best bee for the task at hand. GBC is designed to solve problems iteratively to maximize efficiency in any critical situation. Bee swarms are classified into three categories: employed, onlooker, and scout bees [19]. The employed bee searches for fresh food sources. The scout bee's job is to use a fitness quotient to randomly look for employed bees in specific areas. The assignment is random. If the newly discovered food outperforms previous results, bees will gather in the new area. Bees that are continuously employed search for the ideal places to gather food. Based on the quantitative aspect of food availability, the onlooker bee is responsible for selecting the optimal food source. Initialization, Employed Bee Phase (EBP), Onlooker Bee Phase (OBP), and Scout Bee Phase (SBP) are the four main steps in the technique [20]. The three key steps of the method are repeated in a loop after the initialization step, until the termination condition is met. The flowchart of GBC algorithm is given in Figure 2.

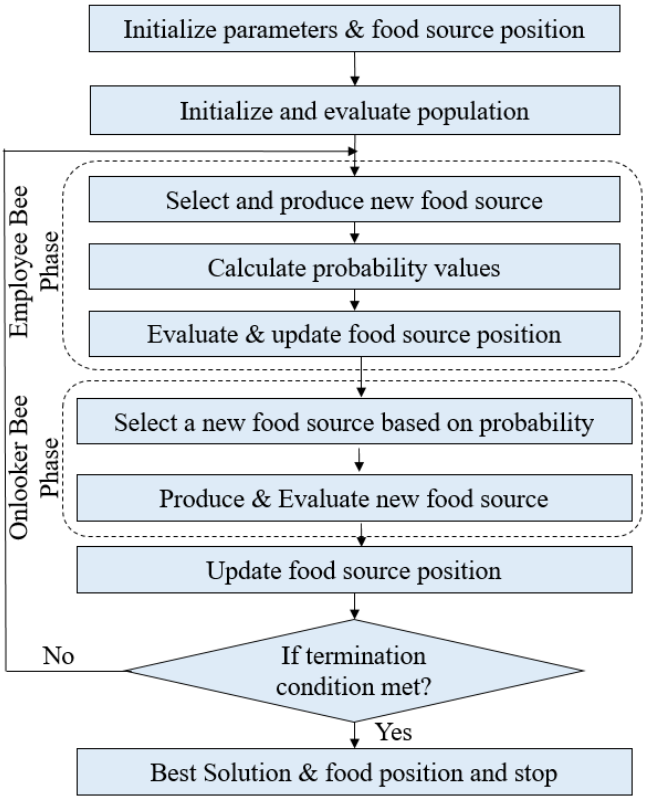

Fig. 2. *Workflow of Genetic Bee Colony*

During the initialization phase, the GBC produces a randomly distributed SN solutions, where SN represents the number of employed or onlooker bees. Let φ denote the i-th food source, with φ being the issue size. Food sources are created within the ith index's limited range $i = 1,2, \dots SN, j = 1,2, \dots D, \varphi_{i,j}$ is a uniformly distributed random real number, with x_{min} and x_{max} indicating the dimension's lower and upper boundaries. A trial counter for each food source is also installed, as seen in Equation (24).

$$x_{i,j} = x_j^{min} + \varphi_{i,j}\left(x_j^{max} - x_j^{min}\right) \qquad (24)$$

Each bee visits a food source during the EBP, and a nearby food supply is established. Where $r1$ represents the randomly chosen index, $x_{r1,j}$ represents the randomly chosen food source that differs from $x_{i,j}$, and r represents the random number from the range generated for each i and j combination, employed bees explore a new solution by conducting a local search around each food source in the manner described below. As stated in Equation (25), greedy selection occurs between $x_{i,j}$ and $v_{i,j}$, with the best option chosen.

Journal of Information Systems Engineering and Management
2025, 10(51s)
e-ISSN: 2468-4376
https://www.jisem-journal.com/

Research Article

$$v_{i,j} = x_{i,j} + \varphi\left(x_{i,j} - x_{r1,j}\right) \quad (25)$$

The onlooker bees choose a food source based on its probability value, which is decided by the amount of nectar available. Equations (24 and 25) are used to estimate the value of the food supply. The fitness value of the solution is calculated for minimization. For maximization, alternative fitness functions are employed, as defined in Equation (27). This roulette wheel-based probabilistic selection, described in Equation (26), increases the likelihood of onlooker bees visiting more promising food sites. As a result, when viable options are available, onlooker bees work hard to discover new potential food sources. When the onlooker bee selects a food source, it creates a new solution. Similar to the EBP, a greedy decision is made between existing and innovative options.

$$p_i = \frac{fit_i}{\sum_{j=1}^{SN} fit_i} \quad (26)$$

$$fit_i = \begin{cases} \frac{i}{1+fit_i} \; fi \geq 0 \\ 1 + abs(fi) \; fi < 0 \end{cases} \quad (27)$$

Each food source includes a trial counter that shows how many times it can't be improved. If a food resource cannot be improved after a certain number of trials during the onlooker and EBPs, the employed bee assigned to that food source becomes a scout. The scout bee employs Equation (24) to find a new food source. By incorporating the SBP, the GBC strategy can quickly escape local minima and boost diversification results. It is worth noting that during the EBP, each food source is thoroughly investigated locally; however, during the OBP, superior food sources are more likely to be discovered. Thus, in the GBC algorithm, the EBP is responsible for diversity, while the OBP is in charge of intensification.

C. Walrus Optimization Algorithm

Walruses eat a variety of aquatic invertebrates. However, the walrus prefers benthic bivalve mollusks, which it acquires via foraging on the sea floor [21]. It searches for and identifies food using its delicate vibrissae and vigorous flipper motions. The walruses search for food, led by the strongest walrus with the largest tusks. The length of the walrus tusks represents the quality of the OF values for potential solutions. As a result, the strongest walrus in the team is the optimal candidate solution with the required OF value. The walruses' search activity leads to the investigation of various sections of the search area, which improves the WaOA's exploration capability in global searches [22]. Using Equations (28) and (29), the process of adjusting walrus positions is mathematically described through the feeding mechanism and guided by the group's most prominent member. This process begins by generating a new position for the walrus using Equation (28). This new position replaces the previous one if it increases the value of the OF.

$$x_{i,j}^{P_1} = x_{i,j} + rand_{i,j} \cdot \left(SW_j - I_{i,j} \cdot x_{i,j}\right) \quad (28)$$

$$X_i = \begin{cases} X_i^{P_1}, F_i^{P_1} < F_i \\ X_i, \quad else \end{cases} \quad (29)$$

In this equation, $x_i^{P_1}$ represents the ith walrus's new position based on the first phase, $x_{i,j}^{P_1}$ represents its jth dimension, $F_i^{P_1}$ represents its OF value, $rand_{i,j}$ represents random numbers, SW denotes the best solution by considering the strongest walrus, and $I_{i,j}$ represents integers randomly selected between 1 and 2. The term $I_{i,j}$is used to improve the algorithm's exploration capacity; a value of 2 causes broader and more significant shifts in the walrus position compared to a value of 1, which is typical for this displacement. These changes facilitate global search by allowing escape from local optima.

A natural behavior of walruses is to move to outcrops or rocky beaches during late summer. This migratory behavior is modeled in WaOA to assist in navigating the search area and identifying favorable positions. Equations (30) and (31) define this mechanism quantitatively. According to the model, each walrus moves to a randomly chosen position in the search region. The new position is computed using Equation (30). If this position improves the OF value, it replaces the original one, as described in Equation (31).

Journal of Information Systems Engineering and Management
2025, 10(51s)
e-ISSN: 2468-4376
https://www.jisem-journal.com/

Research Article

$$x_{i,j}^{P_2} = \begin{cases} x_{i,j} + rand_{i,j} \cdot \left(x_{k,j} - I_{i,j} \cdot x_{i,j}\right), F_k < F_i \\ x_{i,j} + rand_{i,j} \cdot \left(x_{i,j} - x_{i,j}\right), else \end{cases} \quad (30)$$

$$X_i = \begin{cases} X_i^{P_2}, F_i^{P_2} < F_i \\ X_i, \quad else \end{cases} \quad (31)$$

In this context, $x_i^{P_2}$ represents the i-th walrus's new position from the second phase, $x_{i,j}^{P_2}$ is its jth dimension, $F_i^{P_2}$ is its OF value, $X_k, k \in \{1, 2, \ldots, N\}$ and $k \neq i$ is the location of the selected walrus towards which the ith walrus migrates, $x_{k,j}$ is its j-th dimension, and F_k is its OF value.

Walruses are frequently targeted by predators such as polar bears and killer whales. The evasion and defensive mechanisms they employ cause shifts in their positions near their current locations. Simulating this behavior enhances WaOA's exploitation capability during local searches for candidate solutions. Because this behavior involves local movement, the WaOA defines a walrus-centered neighborhood with a specific radius. As global exploration is emphasized during early iterations to locate the optimal region in the search area, the neighborhood radius starts at a maximum value and gradually decreases with each iteration. Thus, local lower and upper bounds are used to define the radius during successive iterations dynamically. In WaOA, this behavior is replicated by forming a neighborhood around each walrus and using equations (31) and (32) to select a new position within this region randomly. As stated in equation (33), the new position replaces the old one if it yields a higher OF value.

$$x_{i,j}^{P_3} = x_{i,j} + \left(lb_{local,j}^t + \left(ub_{local,j}^t - rand \cdot lb_{local,j}^t\right)\right) (31)$$

$$Local\ bounds: \begin{cases} lb_{local,j}^t = \frac{lb_j}{t} \\ ub_{local,j}^t = \frac{ub_j}{t} \end{cases} \quad (32)$$

$$X_i = \begin{cases} X_i^{P_3}, F_i^{P_3} < F_i \\ X_i, \quad else \end{cases} \quad (33)$$

Here, $X_i^{P_3}$ denotes the newly created position for the i-th walrus, $x_{i,j}^{P_3}$ is its j-th dimension, $F_i^{P_3}$ is its OF value, t represents the iteration count,ub_j and lb_j represents the upper and lower bounds for the j-th variable, $ub_{local,j}^t$ and $lb_{local,j}^t$represents the local upper and lower bounds at iteration t, respectively. The workflow of the WaOA is illustrated in Figure 3.

Journal of Information Systems Engineering and Management
2025, 10(51s)
e-ISSN: 2468-4376
https://www.jisem-journal.com/

Research Article

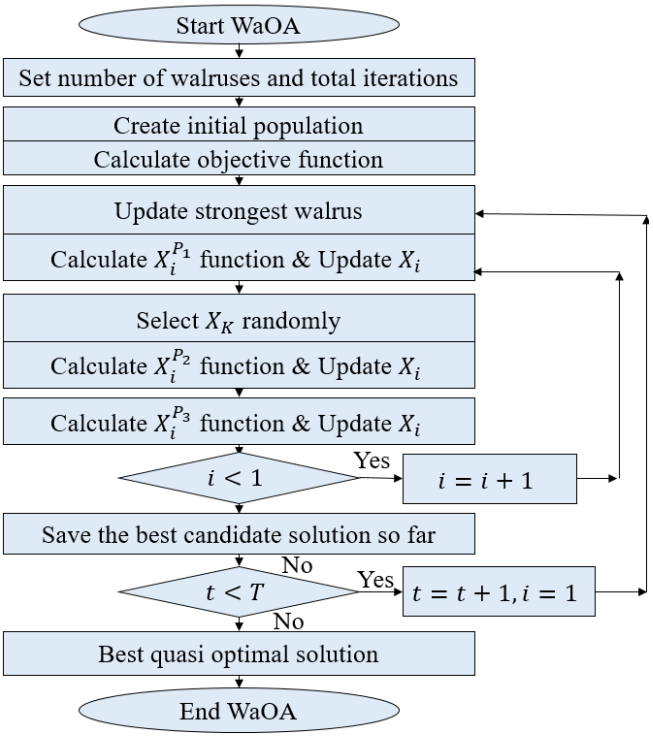

Fig. 3. *Workflow of Walrus Optimization Algorithm*

4. RESULTS

The research aims to optimize IMRT using metaheuristic algorithms for delivering the required dose to the tumor and a minimal dose to the OARs under motion uncertainty. The optimization techniques, such as GBC, SMO, and WaoA, are used to optimize IMRT for lung cancer. For treating the tumor present in the lung, the OARs are the left lung, heart, and spinal cord.

The experiment was carried out in MATLAB software. The motion uncertainty model derived in Section II is used to evaluate the optimization-based IMRT. The conventional IMRT without optimization and the three metaheuristic optimization techniques, like GBC, SMO, and WaoA are compared in terms of the dose (Gy) delivered to the tumor and OARs. First, the dose applied to the tumor is evaluated under breathing motion uncertainty. Figure 4 shows the Tumor DVH under motion uncertainty. The minimum dose required for the tumor is set to 72 Gy, which is represented as a black dotted line. The maximum allowable dose is 80 Gy, and the gray curve shows the IMRT without optimization. The GBC, SMO, and WaoA are represented as blue, green, and red colors. The IMRT without optimization will send a dose of more than 80 Gy to the tumor, while the metaheuristic techniques maintain the dose within 80 Gy.

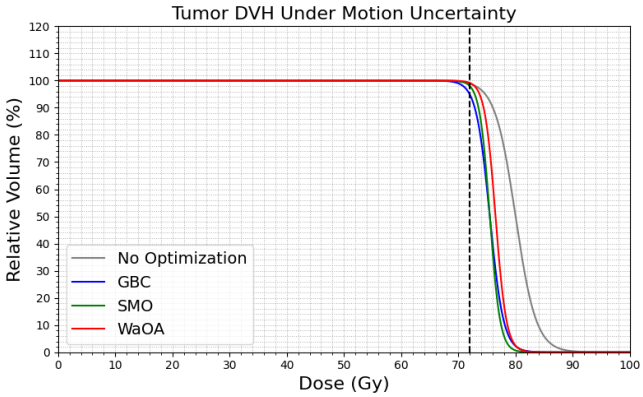

Journal of Information Systems Engineering and Management
2025, 10(51s)
e-ISSN: 2468-4376
https://www.jisem-journal.com/

Research Article

Fig. 4. *Evaluating Tumor DVH under motion uncertainty*

Next, the evaluation was done on the OARs to determine how much dose is delivered to them. It is also important because radiation delivered to other organs can lead to additional problems. The first OAR is the lung, where the tumor is present. The DVH of the lung under motion uncertainty is evaluated and given in Figure 5. The DVH analysis of other OARs, like the heart and spinal cord, is provided in Figures 6 and 7. Similar to the previous task, the same colors are used to differentiate each technique. By analyzing the figures, it is observed that the IMRT without optimization delivers more dose to the lung and other organs when compared to the other three techniques. Comparing the optimization techniques, the SMO delivers the minimum dosage to the OARs.

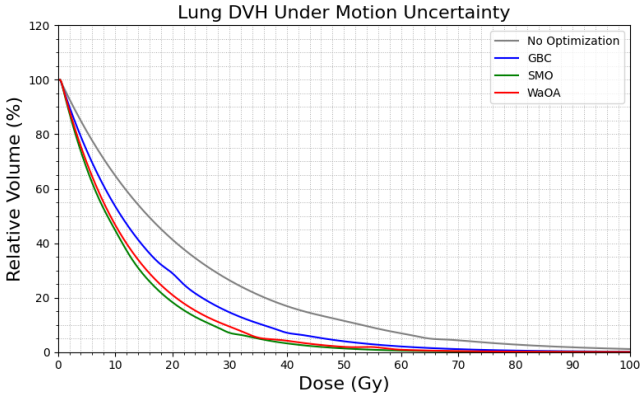

Fig. 5. *Evaluating Lung DVH under motion uncertainty*

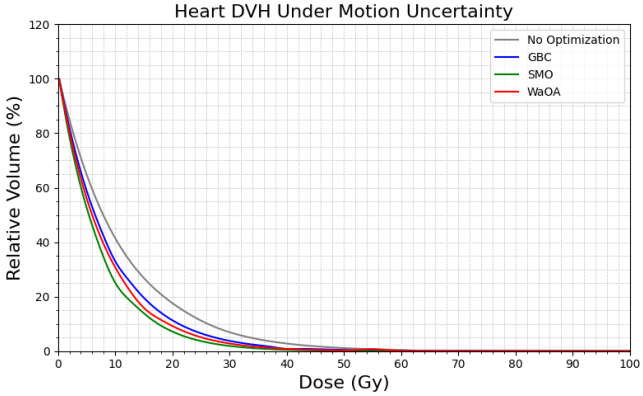

Fig. 6. *Evaluating Heart DVH under motion uncertainty*

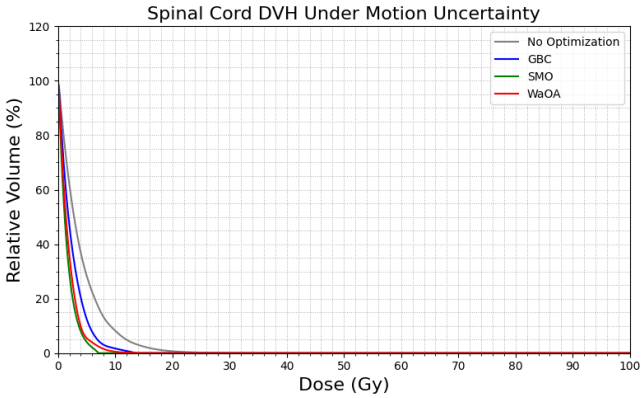

Fig. 7. *Evaluating Spinal Cord DVH under motion uncertainty*

Journal of Information Systems Engineering and Management
2025, 10(51s)
e-ISSN: 2468-4376
https://www.jisem-journal.com/

Research Article

All algorithms are mathematically validated using Table I, which shows the mean dose delivered to the tumor by IMRT with and without optimization. The minimum dose prescribed is 72 Gy. The IMRT without optimization gives 73.4 Gy, while the other two optimizations, SMO and WaoA, give doses of 72.3 Gy and 72.7 Gy, respectively. However, the GBC gives a dose slightly lower than 72 Gy. Based on the prescribed dose, the percentage is calculated using the Equation (34) and is given in Table I. Next, the mean dose delivered to the OARs (lung, heart, spinal cord) is calculated and given in Tables II, III, and IV. The percentage is calculated by taking the maximum dose as the prescribed dose and applying it to Equation (34).

$$Percentage = \frac{Delivered\ Dose}{Prescribed\ Dose} * 100 \qquad (34)$$

TABLE I. *MEAN DOSE DELIVERED ON TUMOR TISSUE UNDER MOTION UNCERTAINTY*

IMRT Techniques	Dose (Gy)	Percentage
No optimization	73.4	101.94
GBC	71.6	99.44
SMO	72.3	100.42
WaOA	72.7	100.97

TABLE II. *MEAN DOSE DELIVERED ON LUNG TISSUE UNDER MOTION UNCERTAINTY*

IMRT Techniques	Dose (Gy)	Percentage
No optimization	46	100
GBC	38	82.61
SMO	31	67.39
WaOA	34	73.91

TABLE III. *MEAN DOSE DELIVERED ON HEART TISSUE UNDER MOTION UNCERTAINTY*

IMRT Techniques	Dose (Gy)	Percentage
No optimization	36	100
GBC	29	80.56
SMO	22	61.11
WaOA	25	69.44

TABLE IV. *MEAN DOSE DELIVERED ON SPINAL CORD TISSUE UNDER MOTION UNCERTAINTY*

IMRT Techniques	Dose (Gy)	Percentage
No optimization	29	100

Journal of Information Systems Engineering and Management
2025, 10(51s)
e-ISSN: 2468-4376
https://www.jisem-journal.com/

Research Article

GBC	24	82.76
SMO	19	65.52
WaOA	21	72.41

By analyzing all the tables, it is observed that the dose delivered without optimization is maximum compared to the other three techniques. Among the three optimization techniques, the SMO delivers the minimum dose to the OAR regions. The experiment results help to conclude that SMO is the most suitable technique to optimize IMRT for lung tumors under motion uncertainty, as it delivers the prescribed dose of 72 Gy to the tumor while also reducing the radiation to the OAR regions. This helps to eradicate the tumor with minimal effect on other organs.

5. DISCUSSION

The research aims to develop an effective IMRT technique for lung cancer treatment, even under motion uncertainty caused by respiration. The mathematical function for IMRT is carefully designed by considering respiratory motion. This motion can reduce the dose delivered to the tumor and may sometimes lead to increased radiation exposure to healthy organs. To ensure effective dose delivery, IMRT is optimized using metaheuristic algorithms such as Starling Murmuration Optimization (SMO), Genetic Bee Colony (GBC), and Walrus Optimization Algorithm (WaOA). To identify the best among these, the experiment is conducted in MATLAB, assuming the prescribed tumor dose is 72 Gy. The DVH is utilized to evaluate the performance of IMRT with all three optimization algorithms as well as without optimization. The results show that optimization significantly reduces the dose delivered to OAR while delivering the required dose to the tumor, compared to conventional IMRT. Among the methods tested, SMO is identified as the most effective for lung cancer treatment.

This research considers only motion uncertainty; however, in practical scenarios, other challenges such as anatomical changes and imaging uncertainty due to low-resolution scans can also affect treatment accuracy. These factors may reduce the effectiveness of the proposed SMO-based IMRT. Future research will aim to address anatomical and imaging uncertainties. The current study is evaluated in the MATLAB environment, and the dataset is obtained from public online sources. Future work will focus on validating the model using real-time clinical datasets.

Conflict of interest: The authors declare no conflicts of interest.

Funding information: The authors declare that there is no funding to be acknowledged.

REFRENCES

[1] Li, Chao, Shaoyuan Lei, Li Ding, Yan Xu, Xiaonan Wu, Hui Wang, Zijin Zhang, Ting Gao, Yongqiang Zhang, and Lin Li. (2023).Global burden and trends of lung cancer incidence and mortality. *Chinese Medical Journal* 136, no. 13 : 1583-1590. DOI: 10.1097/CM9.0000000000002529

[2] Mercieca, Susan, José SA Belderbos, and Marcel van Herk. (2021).Challenges in the target volume definition of lung cancer radiotherapy. *Translational lung cancer research* 10, no. 4: 1983-1998. DOI: 10.21037/tlcr-20-627.

[3] Bosmans, Geert, Angela van Baardwijk, André Dekker, Michel Öllers, Liesbeth Boersma, André Minken, Philippe Lambin, and Dirk De Ruysscher.(2006). Intra-patient variability of tumor volume and tumor motion during conventionally fractionated radiotherapy for locally advanced non-small-cell lung cancer: a prospective clinical study." *International Journal of Radiation Oncology* Biology* Physics* 66, no. 3: 748-753. DOI: 10.1016/j.ijrobp.2006.05.022.

[4] Seppenwoolde Y, Shirato H, Kitamura K, et al.(2002). Precise and real-time measurement of 3D tumor motion in lung due to breathing and heartbeat, measured during radiotherapy. *Int J Radiat Oncol Biol Phys*.53:822–834. DOI: 10.1016/s0360-3016(02)02803-1.

[5] Wilcox, Samuel, Zhefeng Huang, Jay Shah, Xiaofeng Yang, and Yue Chen. (2025). Respiration-Induced Organ Motion Compensation: A Review. *Annals of Biomedical Engineering* 53, no. 2 : 271-283. DOI: 10.1007/s10439-024-03630-w.

Research Article

[6] Azalmad, Ahlam, Oussama Nhila, and Mohamed Hilal. (2025). New Study on Optimizing Cervical Cancer Treatment: Dosimetric Comparison of 3D-CRT, IMRT, and VMAT Techniques at Béni Mellal Oncology Center. *Journal of Obstetrics, Gynecology and Cancer Research*.

[7] Jiang, Zejun, Gongsen Zhang, Tao Sun, Guifang Zhang, Xinqiang Zhang, Xiangyue Kong, and Yong Yin. (2023) .Advantages of IMRT optimization with MCO compared to IMRT optimization without MCO in reducing small bowel high dose index for cervical cancer patients—individualized treatment options. *Translational Cancer Research* 12, no. 12 : 3255-3265. DOI: 10.21037/tcr-22-2792.

[8] Sevilla-Moreno, Andrés Camilo, María Eugenia Puerta-Yepes, Niklas Wahl, Rafael Benito-Herce, and Gonzalo Cabal-Arango.(2025). Interval Analysis-Based Optimization: A Robust Model for Intensity-Modulated Radiotherapy (IMRT). *Cancers* 17, no. 3 : 504. DOI: 10.3390/cancers17030504.

[9] Sevilla, Andrés C., Gonzalo Cabal, Niklas Wahl, María E. Puerta, and Juan C. Rivera. (2025). A robust optimization model for intensity-modulated radiotherapy: Cheap-Minimax." *Medical physics*. 52(5). 3360-3376. DOI: 10.1002/mp.17709.

[10] Carrasqueira, Pedro, Maria João Alves, Joana Matos Dias, Humberto Rocha, Tiago Ventura, Brigida Costa Ferreira, and M. C. Lopes. (2023) . An automated bi-level optimization approach for IMRT. *International Transactions in Operational Research* 30, no. 1: 224-238. DOI: 10.1111/itor.13068

[11] Wu, Qiuwen, Radhe Mohan, Andrzej Niemierko, and Rupert Schmidt-Ullrich. (2002). Optimization of intensity-modulated radiotherapy plans based on the equivalent uniform dose. *International Journal of Radiation Oncology* Biology* Physics* 52, no. 1 : 224-235. DOI: 10.1016/s0360-3016(01)02585-8.

[12] Bortfeld, Thomas, Steve B. Jiang, and Eike Rietzel. (2004). Effects of motion on the total dose distribution." In *Seminars in radiation oncology*, vol. 14, no. 1, pp. 41-51. DOI: 10.1053/j.semradonc.2003.10.011.

[13] Jiao, Shengxiu, Xiaoqian Zhao, and Shuzhan Yao. (2023). Prediction of dose deposition matrix using voxel features driven machine learning approach." *The British Journal of Radiology* 96, no. 1145: 202-373. DOI: 10.1259/bjr.20220373

[14] Chan, Timothy CY, and Velibor V. Mišić. (2013) Adaptive and robust radiation therapy optimization for lung cancer. *European Journal of Operational Research* 231, no. 3: 745-756.DOI: 10.1016/j.ejor.2013.06.003

[15] Goodenough, Anne E., Natasha Little, William S. Carpenter, and Adam G. Hart.(2017). Birds of a feather flock together: Insights into starling murmuration behaviour revealed using citizen science." *PloS one* 12, no. 6 : e0179277. DOI: 10.1371/journal.pone.0179277

[16] Zamani, Hoda, Mohammad H. Nadimi-Shahraki, and Amir H. Gandomi.(2022). Starling murmuration optimizer: A novel bio-inspired algorithm for global and engineering optimization. *Computer Methods in Applied Mechanics and Engineering* 392: 1146 DOI:10.1016/j.cma.2022.114616

[17] Aydemir, Salih Berkan. (2024). Ideal solution candidate search for starling murmuration optimizer and its applications on global optimization and engineering problems. *The Journal of Supercomputing* 80, no. 3 : 4083-4156. DOI:10.1007/s11227-023-05618-0

[18] Chalotra, Sherry, Sumeet Kaur Sehra, and Sukhjit Singh Sehra. (2016). A systematic review of applications of bee colony optimization. In *2016 International conference on innovation and challenges in cyber security (ICICCS-INBUSH)*, pp. 257-260. DOI: 10.1109/ICICCS.2016.7542297

[19] Bacanin, Nebojsa, and Milan Tuba. (2012). Artificial bee colony (ABC) algorithm for constrained optimization improved with genetic operators. *Studies in Informatics and Control* 21, no. 2 : 137-146. DOI: 10.24846/v21i2y201203

[20] Wahid, Abdul, S. C. Behera, and D. Mohapatra. (2015). Artificial Bee Colony and its Application: An Overview. *International Journal of Advanced Research in Computer Engineering & Technology (IJARCET)* 4, no. 4: 1475-1480.

[21] Trojovský, Pavel, and Mohammad Dehghani. (2023). A new bio-inspired metaheuristic algorithm for solving optimization problems based on walruses behavior. *Scientific Reports* 13, no. 1: 8775. DOI; 10.1038/s41598-023-35863-5

[22] Trojovský, Pavel, and Mohammad Dehghani.(2022). Walrus optimization algorithm: a new bio-inspired metaheuristic algorithm. DOI: 10.21203/rs.3.rs-2174098/v1